An MINLP Model for Integrated Optimization of Layout and Cable Routing for Wind Farms

Jingyao Hu, Jinming Xu, Wenchao Meng, Qinmin Yang and Ignacio E. Grossmann

Abstract—The optimal design of layout and cable routing is crucial in maximizing the financial returns of wind farms. Traditionally, the Wind Farm Layout Optimization (WFLO) and Wind Farm Cable Routing (WFCR) problems are addressed separately or using heuristic methods, leading to suboptimal solutions. In this paper, we propose a Mixed-Integer Nonlinear Program (MINLP) formulation for the integrated optimization of layout and cable routing, incorporating a nonlinear wake model, to maximize the Net Present Value (NPV) of wind farms. Moreover, we employ two reformulation methods: a Big-M reformulation of the MINLP and a reformulation as an Mixed-Integer Quadratically Constrained Program (MIQCP), while improving computational efficiency and ensuring tractability. The global optimum can be guaranteed by solving the Big-M MINLP formulation with BARON, ANTIGONE, and SCIP and by solving the MIQCP formulation with Gurobi. Furthermore, experimental results demonstrate that our proposed model significantly improves the NPV compared to existing models employing a simplified linear wake model or two-stage optimization.

I. INTRODUCTION

The global community is shifting from fossil fuels to sustainable energy to reduce environmental pollution and greenhouse gas emissions. According to recent statistics, global CO₂ emissions from energy consumption and industrial processes have increased steadily, rising from 2.0 Gt in 1990 to 37.6 Gt in 2024, with an average annual growth rate of 10.38% [1]. As a result, wind energy, one of the most abundant renewable energy resources with its high commercialization and pollution-free nature in the electrical generation process, has recently attracted significant attention [2], [3].

In the initial design stage of wind farms [4], two primary challenges are encountered: i) the Wind Farm Layout Optimization (WFLO) problem [5], and ii) the Wind Farm Cable Routing (WFCR) problem [6]. Traditionally, WFLO and WFCR problems are solved separately in a sequential manner [7], which leads to suboptimal solutions. WFLO problems focus on the strategic placement of wind turbines to maximize energy production while accounting for wake effects. The wake effect refers to the region of slower wind speed caused by upstream turbines' aerodynamic interactions, which reduces the energy yield of the downwind turbines. Heuristic optimization algorithms such as genetic algorithms (GA) [8], particle

swarm optimization (PSO) [9], [10], or hybrid GA-PSO [11] are commonly employed to solve WFLO problems with analytical wake models. Also, mathematical programming models are employed to formulate Mixed-Integer Linear Programming (MILP) models for WFLO problems with linearized wake effects [12]. WFCR is usually performed after the layout of the wind farm is finalized, wherein the cost of electrical cable accounts for 15%-30% of the total capital expenditure [13]. Existing approaches solving the WFCR problems can be categorized into three main streams: graph theorybased algorithms, such as Prim's algorithm [14]; heuristic optimization techniques, including GA [15] and PSO [16]; and mathematical programming approaches, such as MILP [17], [18]. In real-world applications, one needs to consider physical constraints, such as the presence of obstacles [19] and the no-cable-crossing rule [20].

However, the above two-stage optimization of WFLO and WFCR is suboptimal, as WFLO tends to disperse turbines to minimize wind interference among them, resulting in longer and more costly cables in the subsequent WFCR stage. There have been several works attempting to employ integrated optimization of WFLO and WFCR to enhance wind farm design. For instance, in [21], an MILP model is developed that accounts for pairwise wake effects, and imposes a number of additional inequalities to strengthen its linear programming relaxation. Likewise, another MILP model considering the combined wake effect is proposed to maximize power generation while minimizing costs and energy loss [22]. Although MILP models can provide relatively efficient solutions, simplifying wake effects to linear models and assuming the property of superposition linearity can result in inaccurate power generation estimates. Heuristic methods are thus typically employed for models incorporating more precise nonlinear wake equations. For instance, a novel heuristic method has been introduced that integrates a local search strategy to concurrently optimize both WFLO and WFCR, leading to an increase of up to 12 million euros in the Net Present Value (NPV) of wind farms

Additionally, a hybrid technique, integrating an improved colony algorithm with the genetic algorithm, the dual simplex method, and Kruskal's algorithm, has been developed for joint optimization of turbine placement and cable routing with obstacle avoidance in challenging terrains [24]. A combined framework based on the Non-dominated Sorting Genetic Algorithm II (NSGA-II) and the MILP [25] has also been proposed to optimize the layout of wind turbine locations, connection points, and cable paths. Furthermore, A bilevel non-uniform optimization approach is proposed [26] to conduct integrated

J. Hu, J. Xu, W. Meng and Q. Yang are with the College of Control Science and Engineering, Zhejiang University, Hangzhou, China. E-mails: {jingyao_hu, jimmyxu, wmengzju, qmyang}@zju.edu.cn

IE. Grossmann are with the Department of Chemical Engineering, Carnegie Mellon University, Pittsburgh, USA. E-mails: grossmann@cmu.edu

optimization to minimize the levelized energy cost (LCOE). A nonlinear mathematical programming model with a 3D Gaussian wake model is proposed [27] to optimize the turbine locations and cable layouts with initial solutions obtained via GA and the Prim algorithm. However, due to the use of heuristic methods, all the abovementioned studies cannot guarantee the global optimal solution for the integrated optimization.

In this paper, we present a Mixed-Integer Nonlinear Program (MINLP) formulation for the integrated optimization of WFLO and WFCR, incorporating a more accurate nonlinear wake model to maximize NPV. To ensure computational efficiency and tractability, we reformulate the model through two methods: a Big-M reformulation of MINLP and a reformulation as an MIQCP. As a result, the global optimal solution can be guaranteed by solving the reformulated problems using BARON [28], ANTIGONE [29], and SCIP [30] for the Big-M MINLP formulation, and using Gurobi [31] for the MIQCP formulation. The main contributions of this work are summarized as follows:

- We establish an MINLP formulation with a more accurate nonlinear wake model for the integrated optimization of layout and cable routing for wind farms.
- The Big-M reformulation method is proposed to make the original MINLP problem into a tractable form, enabling solution by state-of-the-art global optimization solvers such as BARON [28], ANTIGONE [29], and SCIP [30].
- The further reformulation as an MIQCP is proposed to effectively improve the computation efficiency and guarantee the global optimal result by Gurobi [31].
- The solution comparisons with optimization without wake effect, integrated optimization with simplified linear wake model, and two-stage optimization, show that our proposed model leads to improvements of 33.64%, 22.8%, and 7.5% of the NPV, respectively.

The remainder of this paper is organized as follows. The problem statement is given in Section II, followed by the detailed mathematical formulation of the WFLO and WFCR integrated optimization problem in Section III. Section IV includes the computational comparison with other solvers and other models. We conclude this article in Section V.

II. PROBLEM STATEMENT

In this work, we address the integrated optimization of layout and cable routing within a predefined geographic area and given potential positions for turbine installation. The objective is to maximize the overall economic benefit of the wind farm, while satisfying a set of engineering and operational constraints.

As illustrated in Fig.1, the gray dots represent potential locations for wind turbine installation, denoted by a discrete set V. For each candidate site $i \in V$, a binary decision variable z_i is defined to indicate whether a turbine is installed at that location $(z_i = 1)$ or not $(z_i = 0)$. In addition to turbine placement, the electrical cable connections between turbines and the substation are modeled using two types of binary variables: $y_{ii'}$ indicates whether there is a cable installed between location i and i', and $x_{i'''s}^t$ indicates whether the cable

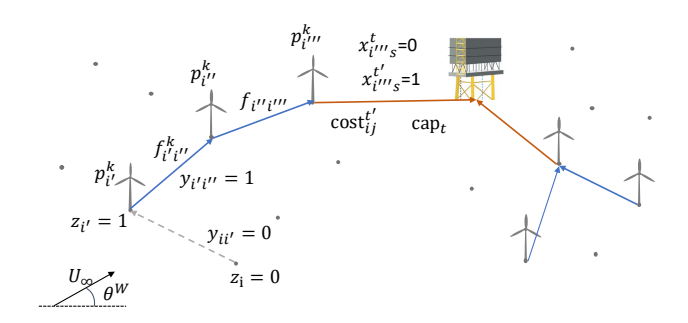


Fig. 1. Example of a layout and cable routing optimization problm

type t is used to connect location i''' and s, where s refers to substation's location. Besides, i, i', i'', i''' represent different possible locations for wind turbines. A set of cable types $t \in T$ are available, each characterized by a specific installation cost $\cot_{ij}^{t'}$ for connecting nodes i and j, and a maximum capacity \cot_{ij}^{t} denoting the maximum current capacity it can support.

To reflect the physical constraints of power generation and transmission, continuous variables are introduced to model the power output of wind turbines and power flow through cables. Specifically, $p_{i'}^k$ represents the power generated by a turbine at location i' under wind scenario $k \in K$, while $f_{i'i''}^k$ denotes the power flow between locations i' and i'' under the scenario k. Each wind scenario k is defined by a specific combination of wind direction θ_k^W and wind speed U_∞^k , derived from historical wind data. These variations influence the wake effects among turbines, affecting their power generation outputs. Besides, the variable $p_{i'}^k$ is non-zero only if a turbine is installed at location i, and both $p_{i'}^k$ and $f_{i'i''}^k$ can be used to guarantee the current balance and cable capacity constraints, which will be detailed in the subsequent section.

Moreover, the optimization model incorporates other key constraints, including bounds on the number of turbines, minimum separation distance between turbines, and topology requirements, among others. Considering all the above components, the optimization model seeks to determine the optimal number and spatial configuration of wind turbines, as well as the cable types and routing strategy for electrical connections. The resulting formulation is an MINLP problem, which captures the combinatorial nature of turbine siting and cable selection and the nonlinearities arising from wake effects and power flow dynamics.

III. MATHEMATICAL FORMULATION

In this section, the wake model is first introduced, and the analytical expression for the wake decay coefficient is derived. Subsequently, distinct power generation strategies for wind turbines operating in different wind speed regions are presented with the Generalized Disjunctive Programming (GDP) approach to handle the piecewise function in power output calculation [32]. Following this, the formulation of the Mixed-Integer Nonlinear Programming (MINLP) model is described. Finally, the proposed reformulation methods are derived, leading to the Big-M MINLP model and Mixed-Integer Quadratically Constrained Programming (MIQCP) model.

A. Wake effect model

Since the position of upstream wind turbines can significantly influence the downstream aerodynamic performances, thereby affecting the power output of downstream wind turbines, the wake effect is a critical factor in evaluating the overall power generation efficiency of a wind farm. The Park model is one of the most widely used wake models as it works well in balancing fidelity and computational cost [33]. In this study, a Park-based multi-variable coupling wake model is used to predict the power generation [34]. As the paper is focused on the layout and cable design optimization, the optimization of the control variables is not considered. Therefore, a greedy control is assumed for every turbine in a wind farm [35]. This means the yaw angle is designed to guarantee that the blade disk planes are perpendicular to the wind direction. Furthermore, the axial induction factor (AIF) is designed to guarantee the power maximization of each turbine by adjusting the blade pitch and generator torque. In the following analysis, α_i and o_i refer to the AIF and the yaw angle of wind turbine i, respectively.

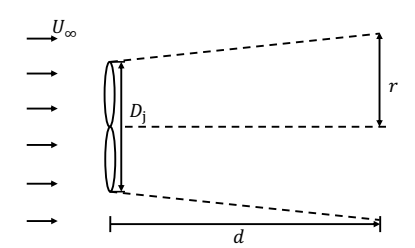


Fig. 2. Wake behind a single turbine

When the wind blows through the disk plane of wind turbine j, the wake effect scale in Fig.2 is measured by a distance d and radius r. The wind speed behind the wind turbine j is expressed as follows:

$$u(d, r, \alpha_j) = (1 - \delta u(d, r, \alpha_j))U_{\infty}, \tag{1}$$

where U_{∞} is the ambient wind speed. $\delta u(d, r, \alpha_j)$ is the wake decay coefficient given by the following expression:

$$\delta u(d, r, \alpha_j) = \begin{cases} 2\alpha_j \left(\frac{R_j}{R(d)}\right)^2, & \text{for any } r \leq R(d), \\ 0, & \text{for any } r > R(d), \end{cases}$$
 (2)

where R_j is the radius of turbine j, equal to the half value of the diameter D_j in Fig. 2, and $R(d) = R_j + \kappa d$ with κ being a wake expansion parameter.

Next, we introduce the wake decay coefficient of wind turbine i influenced by an upstream turbine j, denoted as δu_{ji} . The yaw angle of the upstream turbine reduces the area of the rotor surface perpendicular to the wind flow, so a modification with the cosine function is considered. δu_{ji} is also related to the overlapping area between the wake of the upstream wind turbine and the blade disk planes of the downstream

turbine, which is denoted as $A_{j \to i}^{\text{overlap}}$. In this way, the equation is formulated as follows:

$$\delta u_{ji}(\alpha_j, o_j, \theta^W) = 2\alpha_j \cos(\gamma o_j) \left(\frac{R_j}{R_j + \kappa d_{ij}(\theta^W)}\right)^2 \frac{A_{j \to i}^{\text{overlap}}}{A_i}$$
(3)

where γ is the parameter controlling the sensitivity of the yaw angle, θ^W is the wind direction, A_i is the area of blade disk planes of downstream turbine, and $d_{ij}(\theta^W)$ represents the projection distance of the upstream and downstream turbines along the ambient wind direction θ^W . Fig.3 clearly shows the relationship between the overlapping area and the other parameters.

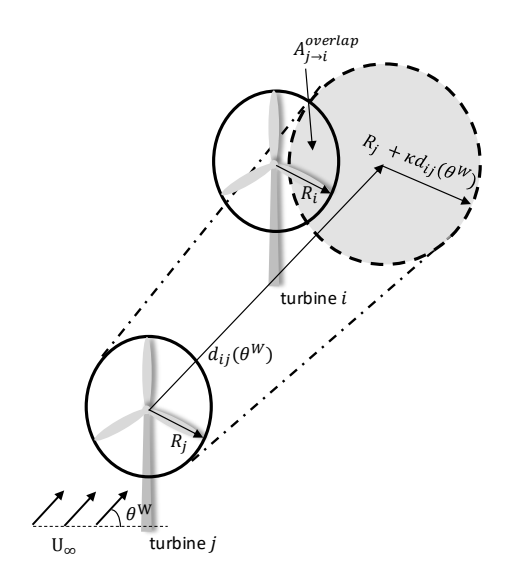


Fig. 3. Diagram of the effect of upstream turbine on downstream turbine

For a wind turbine i influenced by the wake effect of variable upstream wind turbines, the wake decay coefficient is expressed as follows:

$$\begin{split} &\delta u_i(\{\alpha_j, o_j\}_{j \in \mathcal{N}_i}, \theta^W) \\ &= \sqrt{\sum_{j \in \mathcal{N}_i} (\delta u_i(\alpha_j, o_j, \theta^W))^2} \\ &= 2\sqrt{\sum_{j \in \mathcal{N}_i} \left(\alpha_j \cos(\gamma o_j) \left(\frac{R_j}{R_j + \kappa d_{ij}(\theta^W)}\right)^2 \frac{A_{j \to i}^{\text{overlap}}}{A_i}\right)^2}. \end{split}$$

Finally, the wind speed before the downstream wind turbine is expressed as follows:

$$U_i = (1 - \delta u_i(\{\alpha_j, o_j\}_{j \in \mathcal{N}_i}, \theta^W))U_{\infty}.$$
 (5)

It is worth noting that under the greedy control strategy, the control variables are set to o = 0 and $\alpha = \frac{1}{3}$.

B. Power generation model

According to the standard wind turbine power curve shown in Fig. 4, there are typically four distinct regions, each representing a different operational behavior depending on the available wind speed. For the cut-in region, the wind speed is

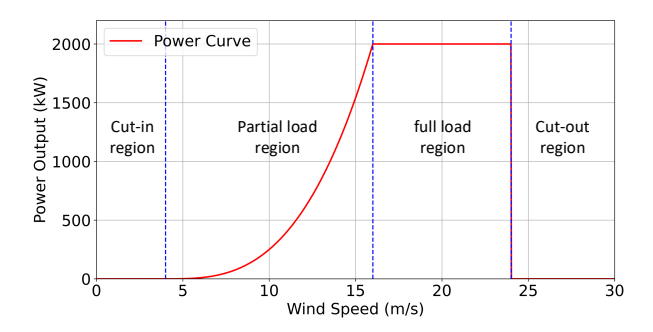


Fig. 4. Example of standard wind turbine power curve

below the cut-in speed, which is too low to generate usable power; it remains stationary or idle. For the partial load region (available wind speed is between the cut-in and rated speed), the following equation is widely used for evaluating the power generation considering the wake effect [36]:

$$P_{i} = \frac{1}{2} \rho A C_{p,i}(\alpha_{i}, o_{i}) U_{i}^{3}$$

$$= \frac{1}{2} \rho A C_{p,i}(\alpha_{i}, o_{i}) ((1 - \delta u_{i}(\{\alpha_{j}, o_{j}\}_{j \in \mathcal{N}_{i}}, \theta^{W})) U_{\infty})^{3},$$
(6)

where ρ and A denote the air density and the rotor area, respectively, U_i represents the wind speed captured by wind turbine i, and $U_i = U_{\infty}$ when there is no wake effect. $C_{p,i}$ is the power coefficient expressed as follows:

$$C_{p,i}(\alpha_i, o_i) = 4\alpha_i(\cos(\beta o_i) - \alpha_i)^2, \tag{7}$$

where β is the coefficient representing the influence of the yaw angle on power generation. For the greedy control strategy with $o_i = 0$ and $\alpha_i = \frac{1}{3}$, the value of power coefficient can be determined by $C_{p,i} = 16/27$.

The turbine operates at its maximum rated capacity for the full load region (available wind speed is between the rated and cut-out speed). Control mechanisms such as pitch regulation or generator torque control, maintain constant output despite increasing wind speed.

The turbine is shut down for the cut-out region to prevent mechanical damage and to ensure safety. No power is generated in this region. To sum up, the power generation of a turbine is expressed by the following piecewise function:

$$U_i = U_{\infty}(1 - \delta u_i(\{\alpha_j, o_j\}_{j \in \mathcal{N}_i}, \theta^W)), \tag{8}$$

$$P_{i} = \begin{cases} 0, & U_{i} < U_{\text{in}}, \\ \frac{1}{2} \rho A C_{p} U_{i}^{3}, & U_{\text{in}} \leq U_{i} < U_{\text{rate}}, \\ \frac{1}{2} \rho A C_{p} U_{\text{rate}}^{3}, & U_{\text{rate}} \leq U_{i} < U_{\text{out}}, \\ 0, & U_{i} \geq U_{\text{out}}, \end{cases}$$
(9)

where $U_{\rm in}$, $U_{\rm rate}$, $U_{\rm out}$ represent the cut-in, rated, and cut-out speeds of wind turbines, respectively.

C. Model formuation

In this section, a Mixed-Integer Nonlinear Program (MINLP) formulation is proposed for the integrated optimization of layout and cable routing. It determines a feasible allocation of turbines and cable connections between all wind turbines and the given substations, maximizing the economic benefit. The model considers the following constraints:

- (a) There is a limit for the number of installed turbines with a minimum N_{\min} and a maximum N_{\max} .
- (b) There is a minimum separation distance D_{\min} between any pair of installed turbines, which avoids the safety problem of blade clash or strong turbulence.
- (c) There is a maximum number of incoming arcs in the substation, $C_{\max,s}$, which denotes the corresponding limit for substation s.
- (d) There are different maximum current capacities that different cable types can support. cap_t denotes the maximum current capacity of cable type t.
- (d) The topology of the built cables must be rooted at the substation, with exactly one cable exiting each turbine.

Moreover, the model involves the following parameters:

- V, the set of possible positions for wind turbine construction.
- K, the set of possible wind scenarios with different combinations of (θ_k^W, U_∞^k) .
- S, the set of positions for substations; s denotes the substation, s ∈ S.
- T, the set of different cable types; t denotes the cable type, $t \in T$.
- H, one year's average of effective power generation time of the wind farm.
- π^k , the probability of wind scenario $k, k \in K$.
- OPEX_{unit}, the maintenance cost per MW of a wind turbine
- dist_{ij} , the distance between positions i and j.
- cost_{wt}, the unit investment cost for one wind turbine.
- $cost_{ij}^t$, the cost of connecting positions i and j, which is calculated by multiplying the unit cost of cable t and dist_{ij}.
- p_{kwh} , the unit electricity price.

Furthermore, the binary variables z_i , y_{ij} , x_{ij}^t and nonnegative continuous variables f_{ij}^k , P_i^k are defined for the proposed MINLP model:

- z_i : = 1 if a turbine is located at position i, and = 0 otherwise. By definition, $z_s = 1$, means a substation is located at position s.
- y_{ij} : = 1 if the directed connection (i, j) is built, and = 0 otherwise.
- x_{ij}^t : = 1 if the directed connection (i, j) is built with a cable type t, and = 0 otherwise;
- f_{ij}^k: the electrical current that flows on the directed cable connection (i, j) for wind scenario k;
- P_i^k : the power generation of position i for the wind scenario $k \in K$.

In order to maximize the economic benefit, the net present value (NPV) is used to estimate the net profit earned by a wind farm over its operational life. The NPV is composed of the annual energy production (AEP), the operating expenditure (OPEX), and the capital expenditure (CAPEX). Based on Equations (4) and (6), and considering the selection of wind turbine installation, P_i^k is expressed as follows:

$$U_i^k = U_{\infty} \left[1 - \sqrt{\sum_{j \in V} (\delta u_{ji}^k z_j)^2} \right], \tag{10}$$

$$P_{i}^{k} = \begin{cases} 0, & U_{i}^{k} < U_{\text{in}}, \\ \frac{1}{2} \rho A C_{p} U_{i}^{k3} z_{i}, & U_{\text{in}} \leq U_{i}^{k} < U_{\text{rate}}, \\ \frac{1}{2} \rho A C_{p} U_{\text{rate}}^{3} z_{i}, & U_{\text{rate}} \leq U_{i}^{k} < U_{\text{out}}, \\ 0, & U_{i}^{k} \geq U_{\text{out}}, \end{cases}$$
(11)

where δu_{ji}^k refers to the wake decay coefficient of wind turbine i influenced by turbine j for wind scenario k. The piecewise function (11) can be formulated as the disjunction (12) in Generalized Disjunctive Programming (GDP) [37], [38]:

$$\begin{bmatrix} B_{i,1}^{k} \\ U_{i}^{k} \leq U_{\text{in}} \\ P_{i}^{k} = 0 \end{bmatrix}$$

$$\stackrel{\vee}{=} \begin{bmatrix} B_{i,2}^{k} \\ U_{\text{in}} \leq U_{i}^{k} < U_{\text{rate}} \\ P_{i}^{k} = \frac{1}{2} \rho A C_{p} U_{i}^{k3} z_{i} \end{bmatrix}$$

$$\stackrel{\vee}{=} \begin{bmatrix} B_{i,3}^{k} \\ U_{\text{rate}} \leq U_{i}^{k} < U_{\text{out}} \\ P_{i}^{k} = \frac{1}{2} \rho A C_{p} U_{\text{rate}}^{3} z_{i} \end{bmatrix}$$

$$\stackrel{\vee}{=} \begin{bmatrix} B_{i,4}^{k} \\ U_{i}^{k} \geq U_{\text{out}} \\ P_{i}^{k} = 0 \end{bmatrix}, i \in V, k \in K,$$

$$B_{i,j}^{k} \in \{ \text{ True, False } \}, j = 1, 2, 3, 4.$$

The AEP of a wind farm is expressed as follows:

$$AEP = H \cdot \sum_{k \in K} \pi^k \cdot \sum_{i \in V} P_i^k.$$
 (13)

The OPEX in a wind farm refers mainly to the annual maintenance cost, and is defined as follows:

$$OPEX = OPEX_{unit} \cdot H \cdot P_r \sum_{i \in V} \cdot z_i, \tag{14}$$

where P_r is the rated power.

The CAPEX in a wind farm is mainly composed of the investment cost of the wind turbines and the cable installation:

$$CAPEX = \sum_{i \in V} cost_{wt} \cdot z_i + \sum_{i,j \in V \cup S} \sum_{t \in T} cost_{i,j}^t \cdot x_{i,j}^t. \quad (15)$$

The NPV is estimated by calculating the annual net income, which is discounted through the interest rate r, and then subtracting the CAPEX. To maximize the NPV, the objective function is given as follows:

$$\max Z = \text{NPV} = \sum_{m=1}^{L} \frac{\text{AEP} \cdot p_{\text{kwh}} - \text{OPEX}}{(1+r)^m} - \text{CAPEX},$$
(16)

where L and r represent the estimated lifetime of the wind farm and the interest rate, respectively.

For a wind turbine built in position $i \in V$ $(z_i = 1)$, the outcoming current equals the incoming current plus the power generation of turbine i. The current balance constraint is then formulated as follows:

$$\sum_{j \in V \cup S, j \neq i} f_{ij}^k = \sum_{j \in V \cup S, j \neq i} f_{ji}^k + P_i^k, \forall i \in V, k \in K. \quad (17)$$

The following cable capacity constraint ensures that enough cable capacity is installed to support the current in each connection:

$$f_{ij}^k \le \sum_{t \in T} \operatorname{cap}_t x_{ij}^t, \forall i, j \in V \cup S, k \in K.$$
 (18)

Equation (19) enforces single-cable-type selection per connection, while Equation (20)-(21) generate radial topology by restricting outdegrees. Note that the out-degree of every installed turbine is set to 1, or 0 otherwise, and the out-degree of every substation is set to 0.

$$y_{ij} = \sum_{t \in T} x_{ij}^t, \forall i, j \in V \cup S.$$
 (19)

$$\sum_{i} y_{ij} \le z_i, \forall i \in V, j \in V \cup S.$$
 (20)

$$\sum_{i} y_{si} = 0, \forall s \in S, i \in V \cup S.$$
 (21)

The following Equation introduces $C_{\max,s}$ as a quantifiable threshold for substation inflow, integrating grid stability into topology design.

$$\sum_{i \in V} y_{is} \le C_{\max,s}, \forall s \in S.$$
 (22)

The limit on the number of installed turbines is imposed to balance cost and redundancy:

$$N_{\min} \le \sum_{i \in V} z_i \le N_{\max}.$$
 (23)

The minimum distance between wind turbines i and j is ensured by the following constraint::

$$z_i + z_j \le 1, \forall i, j \in V, i < j, \operatorname{dist}_{ij} \le D_{\min}.$$
 (24)

The following constraint avoids any crossover between two cables, where the set \mathcal{X} stores pairs of crossover cables $\{(i,j),(h,l)\}.$

$$y_{ij} + y_{ji} + y_{hl} + y_{lh} \le 1, \{(i,j), (h,l)\} \in \mathcal{X}.$$
 (25)

The remaining constraints define all the binary and continuous variables, and fix to the zero value of part of them when they correspond to infeasible choices.

$$x_{ij}^t \in \{0, 1\}, \forall i, j \in V \cup S, t \in T.$$
 (26)

$$z_i \in \{0, 1\}, \forall i \in V. \tag{27}$$

$$y_{ij} \in \{0, 1\}, \forall i, j \in V \cup S.$$
 (28)

$$f_{ij}^k \ge 0, \forall i, j \in V, k \in K. \tag{29}$$

$$f_{jj}^{k} = f_{sj}^{k}, x_{jj}^{t} = y_{jj} = x_{sj}^{t} = y_{sj} = 0,$$

$$\forall s \in S, j \in S \cup V, t \in T, k \in K.$$
 (30)

$$f_{ij}^k, x_{ij}^t = y_{ij} = 0,$$

$$\forall i, j \in V, t \in T, k \in K : \operatorname{dist}_{ij} \leq D_{\min}.$$
 (31)

It is worth noting that the Big-M reformulation is one of the common strategies to reformulate the disjunction as a mixed-integer programming equation [38]. In this study, the model is formulated in Python and is based on the open-source algebraic modeling language Pyomo [39]. Thus, the disjunction (12) can be transformed by Pyomo.GDP extension to mixed-integer linear and nonlinear constraints [40]. To summarize, the mathematical formulation of the layout and cable optimization problem, given by Equations (10)-(31), is a nonconvex MINLP problem.

D. Model reformulation

The original MINLP problem cannot be solved directly by solvers because of its complex structure. Therefore, we propose the following reformulations to enhance the model's tractability and computational efficiency.

Analyzing Equations (10) and (12), it is clear that they involve nonconvexities due to the multiplication of binary variables times continuous variables. Therefore, the Big-M method is adopted to avoid the multiplication of binary variables z_i with nonlinear functions. Thus, the expression of P_i^k during the partial load region ($U_{\rm in} \leq U_i^k < U_{\rm rate}$) is transformed into the following two inequalities:

$$P_i^k \le \frac{1}{2} \rho A C_p U_\infty^3 U_i^{k3} + M_i (1 - z_i), \tag{32}$$

$$0 \le P_i^k \le M_i z_i, \tag{33}$$

where M_i is a sufficiently large parameter. When $z_i=1$, the inequality (32) becomes active as P_i^k takes the largest value for power generation through maximization of the objective function (16); otherwise when $z_i=0$, Equation (33) is active as P_i^k is forced to 0. Thus, Equation (12) is transformed as follows:

$$\begin{bmatrix} B_{i,1}^{k} \\ U_{i}^{k} \leq U_{\text{in}} \\ P_{i}^{k} = 0 \end{bmatrix}$$

$$\stackrel{\vee}{=} \begin{bmatrix} B_{i,2}^{k} \\ U_{\text{in}} \leq U_{i}^{k} < U_{\text{rate}} \\ P_{i}^{k} \leq \frac{1}{2} \rho A C_{p} U_{\infty}^{3} U_{i}^{k3} + M_{i} (1 - z_{i}) \\ 0 \leq P_{i}^{k} \leq M_{i} z_{i} \end{bmatrix}$$

$$\stackrel{\vee}{=} \begin{bmatrix} B_{i,3}^{k} \\ U_{\text{rate}} \leq U_{i}^{k} < U_{\text{out}} \\ P_{i}^{k} = \frac{1}{2} \rho A C_{p} U_{\text{rate}}^{3} z_{i} \end{bmatrix}$$

$$\stackrel{\vee}{=} \begin{bmatrix} B_{i,4}^{k} \\ U_{i}^{k} \geq U_{\text{out}} \\ P_{i}^{k} = 0 \end{bmatrix}, i \in V, k \in K,$$

$$B_{i,j}^{k} \in \{ \text{ True, False } \}, j = 1, 2, 3, 4.$$

$$(34)$$

Therefore, the Big-M MINLP reformulation is defined with the objective function (16), subject to the constraints (10), (13)-(15), (17)-(31), (34). Equation (34) can be transformed by Pyomo.GDP to mixed-integer linear and quadratic constraints, and then the Big-M MINLP model can be solved by global solvers, for example, BARON [28], ANTIGONE [29], and SCIP [30].

However, for medium or large-scale problem sizes, obtaining the global optimum is computationally expensive. To further enhance the optimization efficiency, the Big-M MINLP model is reformulated as an MIQCP, which can be solved more effectively using commercial solvers such as CPLEX [41] and Gurobi [31]. This transformation aims to formulate an exact optimization model that leverages its inherent mathematical structure to enhance computational performance.

In order to derive the quadratic constraints, we first define a new positive continuous variable Z_i that replaces all the square root terms in Equation (32). It is worth noting that $\sum_{j\in V}(\delta u_{ji}^k)^2z_j=\sum_{j\in V}(\delta u_{ji}^k)^2z_j^2$. Then, the following constraint is formulated:

$$Z_i^2 \le \sum_{j \in V} (\delta u_{ji}^k)^2 z_j, \forall i \in V.$$
 (35)

In order to avoid the remaining cubic term in Equation (32), positive continuous variables X_i and Y_i are introduced to define the following two constraints.

$$X_i \le 1 - Z_i, \forall i \in V. \tag{36}$$

$$Y_i \le (1 - Z_i)(1 - Z_i), \forall i \in V.$$
 (37)

Thus, Equation (12) is transformed as follows:

$$\begin{bmatrix} B_{i,1}^{k} \\ U_{i}^{k} \leq U_{\text{in}} \\ P_{i}^{k} = 0 \end{bmatrix}$$

$$\stackrel{\vee}{=} \begin{bmatrix} B_{i,2}^{k} \\ U_{\text{in}} \leq U_{i}^{k} < U_{\text{rate}} \\ P_{i}^{k} \leq \frac{1}{2} \rho A C_{p} U_{\infty}^{3} X_{i} Y_{i} + M_{i} (1 - z_{i}) \\ 0 \leq P_{i}^{k} \leq M_{i} z_{i} \end{bmatrix}$$

$$\stackrel{\vee}{=} \begin{bmatrix} B_{i,3}^{k} \\ U_{\text{rate}} \leq U_{i}^{k} < U_{\text{out}} \\ P_{i}^{k} = \frac{1}{2} \rho A C_{p} U_{\text{rate}}^{3} z_{i} \end{bmatrix}$$

$$\stackrel{\vee}{=} \begin{bmatrix} B_{i,4}^{k} \\ U_{i}^{k} \geq U_{\text{out}} \\ P_{i}^{k} = 0 \end{bmatrix}, i \in V, k \in K,$$

$$B_{i,j}^{k} \in \{ \text{ True, False } \}, j = 1, 2, 3, 4.$$

$$(38)$$

To sum up, the MIQCP is defined with the objective function (16), subject to the constraints (10), (13)-(15), (17)-(31), (35)-(37),(38).

IV. COMPUTATIONAL RESULTS

This section first presents information about the wind farm and then compares the optimization results with different sizes and with different solvers. We also demonstrate the superiority of our established model over the other three models. All models are formulated in Python and are based on the open-source algebraic modeling language Pyomo. Besides, the wake model is implemented in PyTorch, allowing efficient computation of wake decay coefficients between turbines by

leveraging tensor-based modeling. In addition, all examples are implemented on a Linux server running Ubuntu, equipped with 125GB of RAM and an Intel(R) Xeon(R) Silver 4410Y processor. The system has 24 physical cores and 48 logical processors, utilizing up to 8 threads.

A. Wind farm parameters

- 1) Wind farm set-up: The planning size of the wind farm is $5000~\mathrm{m} \times 5000~\mathrm{m}$. Moreover, we consider the Vestas V80 2-MV turbines, each with a diameter of $80\mathrm{m}$ and a hub height of $70\mathrm{m}$. The distance limit between turbines, D_{min} , which is about three to five rotor diameters for a typical turbine, is set to three rotor diameters in this study [21]. The cut-in, rated, and cut-out speeds of the Vestas V80 2-MV turbines are $4\mathrm{m/s}$, $16\mathrm{m/s}$, $24\mathrm{m/s}$, respectively. Moreover, we consider the greedy control strategy of every turbine, which means the control variables are set to o=0 and o=1/3 during simulation. The air density o=1/30 is set as $1.225~\mathrm{kg/m^3}$ 1 like most offshore wind farms. For the parameters related to the wake effect, we refer to the value already optimized based on data from the original paper: o=1.5800, o=
- 2) Wind resource information: The statistical parameters of the wind direction and the wind speed distribution are shown in Table I [42]. The probability mass function $\Pr(\theta_k^W)$ represents the relative occurrence of the discretized wind directions θ_k^W . The corresponding wind speed distribution PDF $(U|\theta_k^W)$ is modeled using the Weibull distribution [43]. We divide the wind speed into six intervals, and based on the parameters in Table I, we can obtain the probability of wind scenario π^k , $k \in K$, |K| = 72. The results are plotted as a wind rose map shown in Fig. 5.
- 3) Other Parameters: The other parameters considered in the model are mainly obtained from the literature and are appropriately adjusted for our model to ensure that the simulation closely reflect real-world conditions [18], [22], [27]. The main economic parameters used in the objective function are given in Table II. We assume that two kinds of cables and two substations have already been installed. The corresponding parameters are shown in Tables III and IV, respectively.

TABLE I
STATISTICAL WIND DATA AT THE TARGET SITE.

k	θ_k^W (°)	$\Pr(\theta_k^W)$	PDF $(U \theta_k^W)$		
			Scale factor λ_k	Shape factor Γ_k	
1	0	0.066	9.98	2.55	
2	30	0.044	8.15	2.35	
3	60	0.043	8.86	2.05	
4	90	0.051	8.65	2.11	
5	120	0.096	10.55	2.28	
6	150	0.114	11.27	2.29	
7	180	0.111	10.94	2.28	
8	210	0.121	11.08	2.23	
9	240	0.115	11.50	2.40	
10	270	0.087	11.28	2.63	
11	300	0.065	10.96	2.74	
12	330	0.089	11.35	2.81	

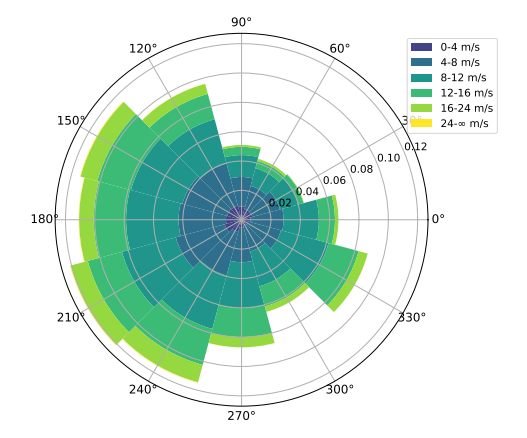


Fig. 5. Wind rose map for wind distribution

TABLE II PARAMETERS RELATED TO COST

Average effective generation time H (h/year)	OPEX _{unit} (\$/KWh)	Turbine investment cost _{wt} (MUSD/each)		
4000	0.02	2.5		
Electrical Price p_{kwh} (\$/KWh)	Project Length L (year)	Interest Rate r (%)		
0.15	25	3		

TABLE III
PARAMETERS RELATED TO CABLES

Cable type	Capacity (KW)	Price (\$/m)
1	2000	135
2	8000	250

TABLE IV
PARAMETERS RELATED TO SUBSTATIONS

Substation index	$C_{\max,s}$	Location (m)
1	4	$ \begin{array}{c} (\frac{1}{3} * 5000, \frac{1}{3} * 5000) \\ (\frac{2}{3} * 5000, \frac{2}{3} * 5000) \end{array} $
2	3	$(\frac{2}{3} * 5000, \frac{2}{3} * 5000)$

B. Comparison of different scale cases

As a benchmark, we evaluate three problem sizes (small, medium, and large) for the integrated optimization problem. Each case varies in: (1) the number of possible turbine positions (25, 49, and 81, respectively), and (2) the maximum number of installable turbines (5, 10, and 15, respectively), while maintaining a minimum installation of 5 turbines. Table V displays the complete problem dimensions. Since the reformulation as an MIQCP introduces additional continuous variables, the number of continuous variables and the number of constraints are reported separately for the Big-M MINLP/MIQCP cases.

The Big-M MINLP model can be solved by specialized global optimization solvers such as BARON [28], ANTIGONE [29], and SCIP [30]. However, these solvers are computationally expensive and typically only feasible for small-scale problems. Our further reformulation as an MIQCP model

TABLE V
THE PROBLEM SIZE OF THREE CASES

Parameters	Case1 (small)	Case2 (median)	Case3 (large)
Possible Positions	25	49	81
Max Turbines	5	10	15
Cont. Vars *	11,749/16,249	37,093/45,913	92,389/106,969
Disc. Vars	8,212	19,612	40,188
Constraints *	35,007/39,507	83,811/92,631	172,183/186,763

Size of Big-M MINLP/MIQCP.

combined with GUROBI [4] can also guarantee globally optimal solutions. We set the relative optimality gap to 0.01 and limit the maximum runtime to 24 hours. The comparative results of these global solvers are presented in Table VI.

For Case 1 with small size, all methods obtained optimal solutions. GUROBI required only 9.1 seconds, demonstrating significant improvements compared to 51.5 minutes for BARON, 25.3 minutes for ANTIGONE, and 116.8 seconds for SCIP. However, when the MIP gap was set to 0.01, GUROBI's solution quality was slightly inferior to that obtained by BARON and SCIP, indicating room for further improvement. Consequently, we included an additional configuration with GUROBI's optimality gap tightened to 0.001, which achieved the optimal solution within 9.4 seconds. For Case 2 with medium size, neither BARON nor ANTIGONE could return feasible solutions within the 24-hour time limit. While SCIP successfully obtained the optimal solution, it required 21 hours of computation time, whereas GUROBI completed the task in just 21.3 minutes. In Case 3 with large size, which represents real-world scenarios, only GUROBI proved capable of solving the problem. With MIP gaps set to 0.01 and 0.001, the obtained objective values are 12.3389 MUSD and 12.3730 MUSD, requiring 18 hours and 19.7 hours of computation time, respectively.

In summary, our proposed Big-M MINLP model can solve minor problems. Further reformulation as an MIQCP can guarantee global optimality and significantly enhance computational efficiency, making it feasible to address practical-scale wind farm layout and cabling planning problems.

C. Integrated optimiztaion with nonlinear wake model

Integrated optimization enables a balanced trade-off between initial investment and long-term power generation revenue, maximizing the wind farm's overall profit. In our study, we employ a nonlinear wake model that more accurately

captures both the intensity of the wake effects and their cumulative effects, allowing for a more precise estimation of energy output. To further demonstrate the significance and practical value of this study, we compare the results of the following four modeling strategies based on the large-scale Case 3 mentioned above.

• Model 1 Integrated optimization without wake effect. If the wake effect is neglected, it is assumed that all wind turbines can fully utilize the ambient wind speed U_{∞} through the optimization process. Thus, the power generation is calculated as follows:

$$P_{i}^{k} = \begin{cases} 0, & U_{\infty}^{k} < U_{\text{in}}, \\ \frac{1}{2} \rho A C_{p} U_{\infty}^{k3} z_{i}, & U_{\text{in}} \leq U_{\infty}^{k} < U_{\text{rate}}, \\ \frac{1}{2} \rho A C_{p} U_{\text{rate}}^{3} z_{i}, & U_{\text{rate}} \leq U_{\infty}^{k} < U_{\text{out}}, \\ 0, & U_{\infty}^{k} \geq U_{\text{out}}. \end{cases}$$
(39)

 Model 2 Integrated optimization with simplified linear wake model. To establish an MILP model, the wake effect is assumed to be linearized and cumulative in [7], [21]. The equation of AEP is expressed as follows:

AEP =
$$H \cdot \sum_{k \in K} \pi^k \cdot (\sum_{i \in V} P_i^k - \sum_{i \in V} \sum_{j \in V} I_{ij}^k y_{ij}),$$
 (40)

where P_i^k is calculated by Equation (39), and I_{ij}^k represents the interference experienced by wind turbine j when a turbine is installed at site i under the wind condition scenario k. In order to ensure the fairness of the comparative study, the following equations are used to calculate I_{ij}^k :

$$I_{ij}^{k} = \begin{cases} 0, & U_{\infty} < U_{\text{in}}, \\ \frac{1}{2} \rho A C_{p} (U_{\infty} \delta u_{ij})^{3}, & U_{\text{in}} \leq U_{\infty} < U_{\text{rate}}, \\ 0, & U_{\text{rate}} \leq U_{\infty}. \end{cases}$$
(41)

- Model 3 Two-stage optimization with nonlinear wake model. The optimization problem is solved in two stages.
 In the first stage, the optimal turbine layout is determined based on simulations that account for nonlinear wake effects. In the second stage, the cable routing is optimized using the fixed turbine positions obtained from the first stage.
- Model 4 Integrated optimization with nonlinear wake model. Based on the optimization model proposed in

TABLE VI
PERFORMANCE COMPARISON OF GLOBAL OPTIMIZATION SOLVERS

Solver	Case 1			Case 2			Case 3		
	Time	NPV (MUSD)	Gap	Time	NPV (MUSD)	Gap	Time	NPV (MUSD)	Gap
BARON 1	51.5min	4.2478	0.01	24h	No feasible sol.	/	24h	No feasible sol.	/
ANTIGONE 1	25.3min	3.9703	0.01	24h	No feasible sol.	/	24h	No feasible sol.	/
SCIP 1	116.8s	4.2478	0.01	21.3h	8.3613	0.01	24h	No feasible sol.	/
GUROBI ²	9.1s	4.2200	0.01	21.0min	8.3236	0.01	18h	12.3389	0.01
GUROBI ²	9.4s	4.2478	0.001	21.3min	8.3614	0.001	19.7h	12.3730	0.001

¹ Big-M MINLP; ² MIQCP;

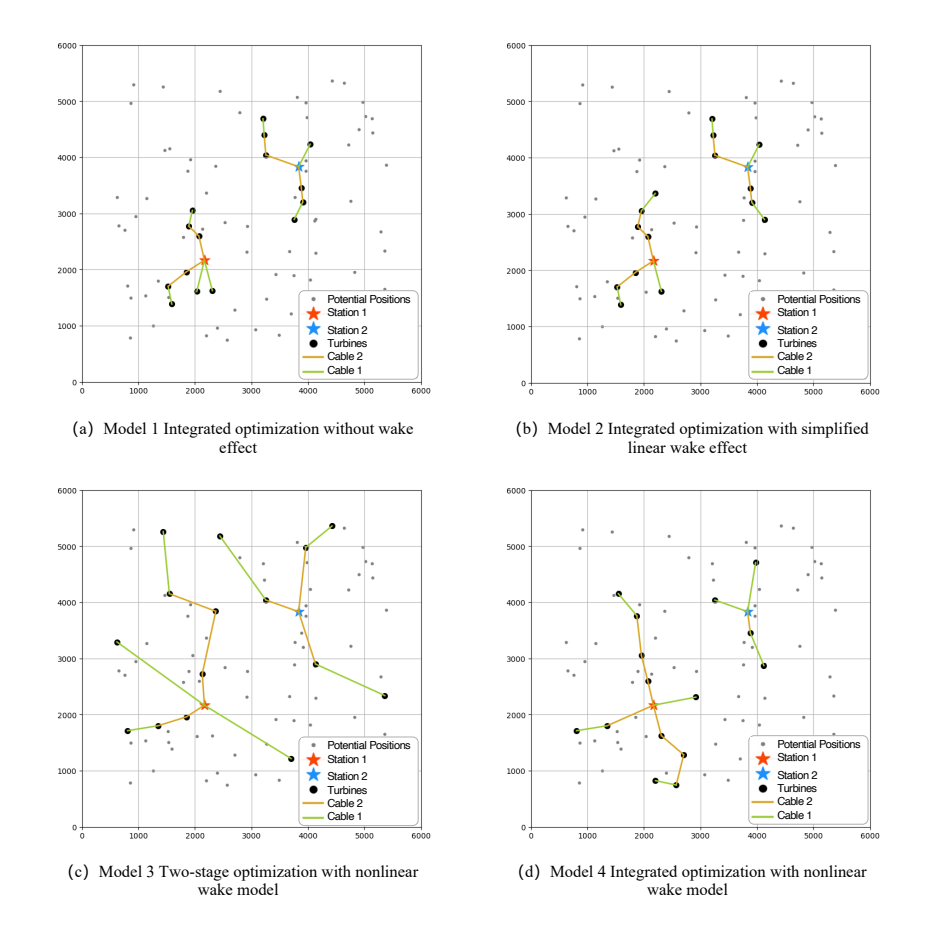


Fig. 6. Optimzal design for Layout and cable rounting result by different models

TABLE VII
RESULTS OF FOUR DIFFERENT MODELS

Model	AEP (kWh)	OPEX (MUSD)	CAPEX (MUSD)	NPV (MUSD)
1 Integrated optimization without wake effect	33,469,458	2.3316	38.6555	8.1653
2 Integrated optimization with simplified linear wake model	33,985,351	2.3316	38.6689	9.4994
3 Two-stage optimization with nonlinear wake model	35,294,702	2.3316	40.2060	11.3823
4 Integrated optimization with nonlinear wake model (Proposed)	35,269,949	2.3316	39.2182	12.3054

this study, the integrated optimization is performed while accounting for the accurate nonlinear wake model.

To ensure a fair comparison, the results of the four models were evaluated under the same nonlinear wake model and with identical parameter settings. The final metrics, including AEP, OPEX, CAPEX, and NPV, are presented in Table VII. The visualization of the wind turbine layout and cable routing results is shown in Fig.6. Since Model 1 neglects wake effects, and the simplified linear wake model in Model 2 tends to underestimate the actual wake effects, the results from Model 1 and Model 2 are similar. Ignoring wake interactions leads to lower-than-expected energy outputs. Although a more compact turbine layout may reduce some CAPEX, the resulting NPV is ultimately lower. The tighter turbine arrangements depicted in Figures 6(a) and 6(b) align with the expectations derived from these two models. Model 3 employs a two-stage optimization. In the first phase, which focuses solely on maximizing power generation, the results tend to favor layouts with turbines

spaced farther apart, where wake effects are less significant (as shown in Figure 6(c)). Consequently, it achieves the highest AEP of 35,269,949 kWh, along with the highest CAPEX of 40.206 million USD compared to the other models. Our proposed Model 4 strikes a better balance between revenue and investment, resulting in the optimal NPV, 12.3054 MUSD, which is 33.64%, 22.8%, and 7.5% higher than Models 1, 2, and 3, respectively. Additionally, the OPEX values across all four models are identical, which is consistent with the fact that the final optimized turbine count reaches the maximum constraint of approximately 15 turbines in each case. To sum up, the integrated optimization of layout design and cable routing, coupled with a nonlinear wake model, is essential for enhancing the economic efficiency of the wind farm.

V. CONCLUSION

In this paper, we have investigated the integrated optimization of the WFLO and the WFCR problems in the wind

farm design stage. Firstly, an MINLP model is formulated by incorporating a nonlinear wake model. In order to enhance the model's tractability, we proposed a Big-M MINLP reformulation. Further reformulation as an MIQCP makes the problem more efficiently solvable with Gurobi, yielding the optimal global solution. Thus, this represents a significant advancement in addressing the integrated design optimization problem with a nonlinear wake model for wind farms.

In future research, we intend to apply decomposition techniques to the existing models to determine the optimal layout and cable routing for large-scale wind farms.

REFERENCES

- International Energy Agency, "Global energy review 2025," https:// www.iea.org/reports/global-energy-review-2025, 2025, iEA, Paris. Licence: CC BY 4.0.
- [2] H. Zhang, A. Tomasgard, B. R. Knudsen, H. G. Svendsen, S. J. Bakker, and I. E. Grossmann, "Modelling and analysis of offshore energy hubs," *Energy*, vol. 261, p. 125219, 2022.
- [3] Q. Wang, C. B. Martinez-Anido, H. Wu et al., "Quantifying the economic and grid reliability impacts of improved wind power forecasting," IEEE Transactions on Sustainable Energy, vol. 7, no. 4, pp. 1525–1537, 2016.
- [4] M. Fischetti, "On the optimized design of next-generation wind farms," European Journal of Operational Research, vol. 291, no. 3, pp. 862–870, 2021
- [5] H. Long and Z. Zhang, "A two-echelon wind farm layout planning model," *IEEE Transactions on Sustainable Energy*, vol. 6, no. 3, pp. 863–871, 2015.
- [6] X. Gong, S. Kuenzel, and B. C. Pal, "Optimal wind farm cabling," *IEEE Transactions on Sustainable Energy*, vol. 9, no. 3, pp. 1126–1136, 2017.
- [7] M. Fischetti, J. Leth, and A. B. Borchersen, "A mixed-integer linear programming approach to wind farm layout and inter-array cable routing," in 2015 American Control Conference (ACC). IEEE, 2015, pp. 5907–5912.
- [8] L. Huang, H. Tang, K. Zhang, Y. Fu, and Y. Liu, "3-d layout optimization of wind turbines considering fatigue distribution," *IEEE Transactions on Sustainable Energy*, vol. 11, no. 1, pp. 126–135, 2018.
- [9] P. Hou, W. Hu, M. Soltani, and Z. Chen, "Optimized placement of wind turbines in large-scale offshore wind farm using particle swarm optimization algorithm," *IEEE Transactions on Sustainable Energy*, vol. 6, no. 4, pp. 1272–1282, 2015.
- [10] P. Hou, W. Hu, M. Soltani, C. Chen, B. Zhang, and Z. Chen, "Offshore wind farm layout design considering optimized power dispatch strategy," *IEEE Transactions on Sustainable Energy*, vol. 8, no. 2, pp. 638–647, 2016.
- [11] Q. Yang, H. Li, T. Li, and X. Zhou, "Wind farm layout optimization for levelized cost of energy minimization with combined analytical wake model and hybrid optimization strategy," *Energy Conversion and Management*, vol. 248, p. 114778, 2021.
- [12] M. Fischetti, M. Fischetti, and M. Monaci, "Optimal turbine allocation for offshore and onshore wind farms," in *Optimization in the Real World: Toward Solving Real-World Optimization Problems*. Springer, 2015, pp. 55–78.
- [13] J. S. González, M. B. Payán, J. M. R. Santos, and A. M. Gonzalez, "A review and recent developments in the optimal wind-turbine micrositing problem," *Renewable and Sustainable Energy Reviews*, vol. 30, pp. 133–144, 2014.
- [14] P. Hou, W. Hu, and Z. Chen, "Offshore substation locating in wind farms based on prim algorithm," in 2015 IEEE Power & Energy Society General Meeting. IEEE, 2015, pp. 1–5.
- [15] F. M. Gonzalez-Longatt, P. Wall, P. Regulski et al., "Optimal electric network design for a large offshore wind farm based on a modified genetic algorithm approach," *IEEE Systems Journal*, vol. 6, no. 1, pp. 164–172, 2011.
- [16] K. Deveci, B. Barutçu, E. Alpman, A. Taşcıkaraoğlu, and O. Erdinç, "Electrical layout optimization of onshore wind farms based on a twostage approach," *IEEE Transactions on Sustainable Energy*, vol. 11, no. 4, pp. 2407–2416, 2019.
- [17] M. Fischetti and D. Pisinger, "Optimizing wind farm cable routing considering power losses," *European Journal of Operational Research*, vol. 270, no. 3, pp. 917–930, 2018.

- [18] A. Cerveira, A. de Sousa, E. J. S. Pires et al., "Optimizing wind farm cable layout considering ditch sharing," *International Transactions in Operational Research*, vol. 31, no. 1, pp. 88–114, 2024.
- [19] D. Cazzaro and D. Pisinger, "Balanced cable routing for offshore wind farms with obstacles," *Networks*, vol. 80, no. 4, pp. 386–406, 2022.
- [20] D. Cazzaro, M. Fischetti, and M. Fischetti, "Heuristic algorithms for the wind farm cable routing problem," *Applied Energy*, vol. 278, p. 115617, 2020.
- [21] M. Fischetti and M. Fischetti, "Integrated layout and cable routing in wind farm optimal design," *Management Science*, vol. 69, no. 4, pp. 2147–2164, 2023.
- [22] D. J. Presser, M. J. Fiorini, and D. C. Cafaro, "Optimization of wind farm layout and cable network topology under generalized wake effects," in *Computer Aided Chemical Engineering*. Elsevier, 2023, vol. 52, pp. 3191–3196.
- [23] D. Cazzaro, D. F. Koza, and D. Pisinger, "Combined layout and cable optimization of offshore wind farms," *European Journal of Operational Research*, vol. 311, no. 1, pp. 301–315, 2023.
- [24] Y. Wu, T. Xia, Y. Wang *et al.*, "A synchronization methodology for 3d offshore wind farm layout optimization with multi-type wind turbines and obstacle-avoiding cable network," *Renewable Energy*, vol. 185, pp. 302–320, 2022.
- [25] J. He, M. Ge, S. D. Žarković et al., "A novel integrated optimization method of micrositing and cable routing for offshore wind farms," Energy, vol. 306, p. 132443, 2024.
- [26] D. Zhang, Z. Liu, Y. Liang et al., "Bilevel optimization of non-uniform offshore wind farm layout and cable routing for the refined lcoe using an enhanced pso," *Ocean Engineering*, vol. 299, p. 117244, 2024.
- [27] Z. Cao, L. Chen, K. Li et al., "A mathematical programming approach for joint optimization of wind farm layout and cable routing based on a three-dimensional gaussian wake model," Wind Energy, vol. 28, no. 2, p. e2960, 2025.
- [28] Nick Sahinidis, BARON user manual v. 2025.3.19. [Online]. Available: https://minlp.com/baron-solver
- [29] R. Misener and C. A. Floudas, "ANTIGONE: algorithms for continuous/integer global optimization of nonlinear equations," *Journal of Global Optimization*, vol. 59, no. 2–3, 2014.
- [30] SCIP: Solving Constraint Integer Programs. [Online]. Available: https://www.scipopt.org/
- [31] Gurobi Optimizer Reference Manual. [Online]. Available: https://docs.gurobi.com/projects/optimizer/en/current/
- [32] I. E. Grossmann, Advanced optimization for process systems engineering. Cambridge University Press, 2021.
- [33] I. Katic, J. Højstrup, and N. O. Jensen, "A simple model for cluster efficiency," in *European wind energy association conference and exhibition*. A. Raguzzi, 1987, pp. 407–410.
- [34] J. Park and K. H. Law, "A data-driven, cooperative wind farm control to maximize the total power production," *Applied Energy*, vol. 165, pp. 151–165, 2016.
- [35] Z. Xu, H. Geng, and B. Chu, "A hierarchical data-driven wind farm power optimization approach using stochastic projected simplex method," *IEEE Transactions on Smart Grid*, vol. 12, no. 4, pp. 3560– 3569, 2021.
- [36] W. Wang, X. Kong, G. Li, X. Liu, L. Ma, W. Liu, and K. Y. Lee, "Wind farm control using distributed economic mpc scheme under the influence of wake effect," *Energy*, vol. 309, p. 132902, 2024.
- [37] F. Trespalacios and I. E. Grossmann, "Review of mixed-integer nonlinear and generalized disjunctive programming methods," *Chemie Ingenieur Technik*, vol. 86, no. 7, pp. 991–1012, 2014.
- [38] R. Raman and I. E. Grossmann, "Modelling and computational techniques for logic based integer programming," *Computers & Chemical Engineering*, vol. 18, no. 7, pp. 563–578, 1994.
- [39] W. E. Hart, C. D. Laird, J.-P. Watson, D. L. Woodruff, G. A. Hackebeil, B. L. Nicholson, and J. D. Siirola, *Pyomo-Optimization Modeling in Python*, ser. Springer Optimization and Its Applications. Springer, 2017, vol. 67.
- [40] B. L. Nicholson, J. D. Siirola, J.-P. Watson, D. L. Woodruff, and W. E. Hart, "Pyomo.gdp: Disjunctive modeling and solving in python," *Computers & Chemical Engineering*, vol. 116, pp. 221–232, 2018.
- [41] User's Manual for CPLEX. [Online]. Available: https://www.ibm.com/docs/en/icos/22.1.1?topic=optimizers-users-manual-cplex
- [42] J. Park and K. H. Law, "Layout optimization for maximizing wind farm power production using sequential convex programming," *Applied Energy*, vol. 151, pp. 320–334, 2015.
- [43] A. J. Hallinan Jr, "A review of the Weibull distribution," *Journal of Quality Technology*, vol. 25, no. 2, pp. 85–93, 1993.